Temperature and hydrological variations during the Late-Glacial in the central Mediterranean: application of the novel ostracod-clumped isotope thermometer.

Marchegiano Marta[1,2*], Peral Marion[2,3], Doyle Rebecca[2], García-Alix Antonio[1], Francke Alexander[4,5], Snoeck Christophe[2], Goderis Steven[2], and Claeys Philippe[2]

1: Departamento de Estratigrafía y Paleontología, Universidad de Granada, 18071 Granada, España

2: Archaeology, Environmental changes and Geo-Chemistry, Vrije Universiteit Brussel, Pleinlaan 2, 1050 Brussels, Belgium.

3 :Environnements et Paléoenvironnements Océaniques et Continentaux (EPOC), Univ. Bordeaux, CNRS, Bordeaux INP, EPOC, UMR 5805, F-33600 Pessac, France

4: Archeology, College of Humanities, Arts and Social Science, Flinders University, 5042 Adelaide, Australia

5: School of Physics, Chemistry and Earth Sciences, Faculty of Sciences, Engineering and Technology, The University of Adelaide, 5005 Adelaide, Australia

**Correspondind author: Marta Marchegiano, martamarchegiano@gr.es*

ABSTRACT

This study shows, for the first time, the absence of a vital effect in the clumped isotope carbonate (Δ_{47}) fossil ostracod signal and confirms the ability of the novel ostracod-Δ_{47}thermometer to reconstruct past temperatures and hydrological conditions in complex lacustrine systems. Furthermore, the application of Δ_{47} analyses on the ostracod species *Candona angulata* and *Cyprideis torosa* from Lake Trasimeno record (central Italy), which today precipitate their shells during the cold and the warm season respectively provides evidence that by combining biological (i.e., ostracod shell precipitation timing), paleontological (i.e., identification of ostracod species) and geochemical (i.e., Δ_{47}) approaches, the ostracod-Δ_{47} thermometer accurately reconstructs past seasonality. Despite the absence of a vital effect, not all species can be combined for Δ_{47} analyses in environments with seasonal temperature variations; only those that precipitate their shells during the same season should be considered. The application of the ostracod-Δ_{47}thermometer on the Trasimeno lacustrine record gives rise to the first continental warm season paleotemperature reconstruction of the last 43 ky in central Mediterranean area. The combination of Δ_{47} and oxygen isotope composition ($\delta^{18}O_{ost}$) measured on ostracod shells provides the isotopic composition of the water from which the carbonate precipitated ($\delta^{18}O_{w}$) and thereby, changes in the evaporation/precipitation balance in this area. Before the Last Glacial Maximum (LGM), equivalent to the Marine Isotopic Stage 3 (MIS3, from 43 to 29ky), warm season temperatures ranged from 15 ± 1.6 °C to 22 ± 2.3 °C, equivalent to 2 to 6 °C colder than today. Hydrological conditions during this period are similar to the present-day ones, characterized by a permanent lake and a high evaporation/precipitation ratio (E/P). The drastic decrease of the warm season temperatures (ranging from 10 ± 2.9 °C to 17 ± 3.1 °C) and of the E/P ratio during LGM and Late-glacial (MIS2, from 29 to 11.6 ky) correspond to the global climate cooling and low summer insolation, suggesting an amplifying role, of the latter, in the effects of the millennial scale climatic variations. At the Pleistocene/Holocene transition, both warm season temperature (25 ± 2 °C) and the E/P ratio increased in conjunction with the summer insolation. During the early Holocene, warm season temperature (23 ± 2 °C) closely resembles present-day values. However, cold season temperature (12 ± 2 °C) is approximately 4 °CC warmer than today. Notably, no hydrological differences are identified between the warm and the cold season underlying a lower seasonality contrast compared to the present, along with enhanced warm season precipitation. The good agreement between the Δ_{47} temperatures reconstructed for the last 1 ky and the temperatures presently recorded at Lake Trasimeno (8 °C cold and

22 °C for warm season), confirms the accuracy of the analyses and the applicability of the ostracod-Δ_{47}thermometer to reconstruct seasonal temperature changes.

KEYWORDS

Carbonate Clumped Isotope, Freshwater ostracods, Paleotemperatures, Paleohydrology, Seasonality, Central Mediterranean.

1. INTRODUCTION

The Intergovernmental Panel on Climate Change (IPCC) considers the Mediterranean region a climate change hotspot (Ali et al., 2022). According to climate projections, the Mediterranean region is expected to warm at a rate approximately 20 % higher than global average. Additionally, it will undergo significant drying, a phenomenon not anticipated in other regions situated at the same latitude (Lionello and Scarascia, 2018). The vulnerability of this region is a consequence of complex and interacting processes related to the landscapes, geographical location, high population density, and long history of human occupation (Ali et al., 2022). Predictive modeling of potential future climate scenarios is key to develop strategies for adaptation and mitigation. To generate these climate projections, the forcing mechanisms driving climate variability across different temporal and geographical scales need to be better understood. Moreover, ancient analogues must validate the forecasted changes scenario. Owning to the Mediterranean's complex topography, each region responds differently to atmospheric and marine climate dynamics (Abrantes et al., 2012). Accurate high-resolution paleoclimatic reconstructions for the different Mediterranean regions are required. Lake sediments certainly constitute one of the best continental archives for developing paleoclimatic and paleoenvironmental reconstructions because they can capture rapid climate changes at regional scales (Gornitz, 2009). Paleotemperature reconstructions have always been assumed to play an important role in understanding climatic variations; however, despite more than half a century of studies, quantitative and well-constrained continental temperature reconstruction remains challenging. The complexity lies in disentangling and quantifying the effects of the various parameters that impact the local climate and environment (e.g., temperature, hydrology, lake structure). Continental quantitative temperature records in the central Mediterranean area remain rare, mainly focussed on the last 15 ky (e.g., Heiri et al., 2015; Larocque and Finsinger, 2008; Robles et al., 2023; Samartin et al., 2017) and most of them are based on transfer functions (e.g., pollen, chironomids, and ostracods). The oldest temperature record comes from the Monticchio lake (southern Italy, Fig.1). It is based on pollen analyses, and provides air temperature of the coldest month (January) from the last ca. 102 ky (Allen et al., 1999). Marchegiano et al. (2020) applied the Mutual Ostracod Temperature Range transfer function (MOTR, Horne, 2007) to ostracod assemblages from Lake Trasimeno (central Italy, Fig.1) to reconstruct air temperature of the warmest (July) and coldest (January) months during the Late Pleistocene. However, this approach produced large temperature ranges (Marchegiano et al., 2020; Fig. 3).

The carbonate clumped isotope (Δ_{47}) technique (Eiler, 2007), currently mostly applied to marine carbonate fossils and sediments (de Winter et al., 2021; Marchegiano and John, 2022; Meinicke et al., 2021; Peral et al., 2020), has the potential to significantly reduces the methodological uncertainties associated with lake paleotemperature measurements. The technique is based on the temperature-dependent abundance of ^{13}C-^{18}O bonds in carbonate minerals. The increased abundance of these bonds in carbonate is associated with decreasing water temperatures, revealing the temperatures at which calcium carbonate ($CaCO_3$) precipitated. The combination of Δ_{47} and $\delta^{18}O$ provide the $\delta^{18}O_w$ and give insight on the hydrological conditions.

The ostracod-Δ_{47} thermometer provides a new tool to reconstruct lacustrine water temperatures, with an accuracy of ~ ± 2 °C (Marchegiano et al., 2023). Marchegiano et al. (2023), showed the applicability of the Δ_{47} technique on ostracod shells as well as the absence of any vital effect (i.e., offset between the isotopic signal of biogenic carbonate and inorganic calcite precipitated under same conditions) on ostracods living at the same temperatures. Ostracods are aquatic micro-crustaceans (size from 0.3 to 5 mm) with a stable bivalve low-Mg calcite shells easily to preserve and thus ideally suited for geochemical analyses (Holmes and De Deckker, 2012). As they grow, they secrete increasingly large carapaces from the ions dissolved in the host water and pass through 8 molting stages before reaching adulthood (Turpen and Angell, 1971). The shell calcification is quick, ranging from a few hours to a few days (Börner et al., 2013), and representative of the geochemical conditions of the environment at that time (Chivas et al., 1983).

This study generates the first ca. 43 ky continental warm season temperature record for the central Mediterranean area by applying the novel ostracod-Δ_{47} thermometer on a ca. 8.9 m long sedimentary core from Lake Trasimeno (central Italy). The Trasimeno sedimentary core has been well analyzed in previous studies (Francke et al., 2022; Marchegiano et al., 2018, 2019, 2020) by using a multiproxy approach (i.e., micropaleontological, sedimentological and geochemical) making this record particularly suitable to apply this novel paleothermometer.

The clumped isotope technique has already been used on fossil ostracods (Song et al., 2022 and Yue et al., 2022), however, no studies ever determined whether a vital effect influences the Δ_{47} signal on fossil ostracods. To fill this gap, Δ_{47} analyses are carried out on two different ostracod species coming from the same sediment sample that lived and precipitated their shells at the same season and temperatures. Also, by combining Δ_{47} with the analyses of the classic oxygen isotopic composition of the ostracod shells ($\delta^{18}O_{ost}$), this study confirms the ability of the ostracod-Δ_{47} thermometer to reconstruct $\delta^{18}O_w$ variations in past lacustrine environments.

1.1 Study site: Lake Trasimeno

Lake Trasimeno (latitude 43°08′N, longitude 12°06′E, 258 m above sea level, Fig. 2) is an endorheic and very shallow lake (max depth of ~6 m and ~4 m in average) with a surface area of 124.3 km^2 located in central Italy (Umbria region). It has a tectonic origin and the lacustrine sedimentation started during the Middle Pleistocene (Gasperini et al., 2010). The catchment area is predominantly represented by Pliocene to Holocene lacustrine and fluvial sandstone and claystone deposits with very few carbonates (Gasperini et al., 2010). Because of its characteristics, the hydrology of the lake strictly depends on climatic and environmental variations. Lake-level fluctuations influence, at the seasonal and annual-decadal scale, the physical-chemical and biological lake properties (Ludovisi and Gaino, 2010). The climate regime is characterized by warm-arid summers and mild-humid winters. Today, water temperatures are close to the atmospheric ones with a difference of 2 - 4 °C during the year. Temperatures are homogeneous along the entire water column due to a continuous mixing facilitated by the shallowness and the very large surface of the lake (Marchegiano et al., 2017). Previous studies (Marchegiano et al., 2018, 2019, 2020 and Francke et al., 2022) showed that, over the last ca. 47 ky, Lake Trasimeno responded rapidly to millennial scale climatic variations associated with Greenland stadial and interstadial events, according to Rasmussen et al. (2016). Low (high) lake levels corresponded to cold (warm) and dry (humid) stadial (interstadial) events. This demonstrates that Lake Trasimeno detects regional as well as global climatic signals. The living and fossil ostracod fauna of Lake Trasimeno have also been studied intensively (Marchegiano et al., 2017, 2018, 2019 and 2020), indicating a prevalence of permanent low saline lake conditions during MIS3 and the Holocene and ephemeral high salinity lake conditions during the MIS2.

Thanks to its strategical position in the central Mediterranean, its high sensitivity to climate and environmental changes and the abundance and great preservation of the ostracod fauna, Lake Trasimeno constitutes the perfect target to test the ostracod-Δ_{47}thermometer in past sedimentary records and reconstruct atmospheric changes in the central Mediterranean.

2. Material and Methods

2.1 Trasimeno core and its chronology

An 8.6 m long sediment core (Co1320; 43° 09.624′N, 12° 03.491′E) (Fig. 2) was retrieved at ~4.9 m water depth from a floating platform using a gravity piston corer (UWITEC®) during a sampling campaign in November 2014. The core was split lengthwise in the laboratory. While one-half was archived and stored at the University of Cologne (Germany), the other half was used for visual lithological inspection and then subsampled at 2-cm intervals for geochemical and micropalaeontological analyses (Marchegiano et al., 2018, 2019, 2020 and Francke et al., 2022).

The chronological model of the Trasimeno core Co1320 has been developed using ten radiocarbon ages (Fig. 3) and ultimately covers the last ca. 47 ky (Marchegiano et al., 2018). This study updates this calibration using a Bayesian age-depth modeling calculated by means of the software rBacon 3.1 (Blaauw et al., 2018; Blaauw and Christen, 2011), and the IntCal 2020 calibration curve (Reimer, 2020) (Fig. 3). rBacon 3.1 software (Blaauw et al., 2018; Blaauw and Christen, 2011) subdivides the core into a series of vertical sections (of thick=5 cm thickness), and it estimates the accumulation rate (years/cm) for each of these sections through millions of Markov Chain Monte Carlo (MCMC) iterations (Fig. 3). The memory defines how much the accumulation rate of a particular depth in a core depends on a depth above it. The age model is then formed combining the accumulation rate with estimated starting dates for the first section (Fig. 3). The bulk organic matter samples at 631 cm (COL3665.1.1) and 154.5 cm (COL3662.1.1) exhibit higher br/(cren+cren0) GDGT ratios, indicating a substantial contribution from soil organic matter (SOM) (Francke et al., 2022). This implies that the incorporation of pre-aged SOM in these samples may distort the bulk ^{14}C age. Consequently, the two samples are excluded from the age-depth model. Considering the limited presence of carbonate bedrock in the catchment area and the high lake surface compared to the water volume ratio that facilitate rapid exchange with the atmosphere, Lake Trasimeno is anticipated to have minimal reservoir and/or hardwater effects on lacustrine organic matter (Francke et al., 2022).

2.2 Carbonate classic and clumped-isotope analyses

For classic and clumped-isotope analyses, we selected a total of 16 samples (Table 1) by combining the results of the ostracod assemblage analyses (Marchegiano et al., 2018 and 2019), the derived MOTR temperature curve (Marchegiano et al., 2020) and the updated age model. These samples correspond to the main temperature and environmental variations along the entire core interval. To reach the required carbonate amount for clumped-isotope analyses (minimum 500 µg per replicate), adjacent subsamples (2 cm thick) (Table 1) deposited during the same climatic event are merged (i.e., all samples belong to the same Glacial stadial or interstadial) (Marchegiano et al., 2018, 2019 and 2020). All subsamples were mixed before performing Δ_{47} analyses. Adult ostracod valves were picked and manually cleaned with a brush under the stereomicroscope to remove any sediments and other possible contaminants (i.e., organic matter). The good state of preservation (i.e., no diagenetic alteration) and cleanliness of the ostracod shells was checked under the scanning electron microscope (SEM) (Fig. 4). Analyses for Δ_{47} and $\delta^{18}O_{ost}$ were carried out on the most abundant species *Cyprideis torosa, Sarcypridopsis aculeata, Eucypris mareotica, Heterocypris salina* and *Candona angulata* (Fig. 4). A total of 40 to 60 valves per replicate is needed to assure sufficient material (500 - 600 µg per replicate), whereby the exact number depends on the species (i.e., size and thickness of the shells). Each sample is replicated from 5 to 15 times (300 - 1000 valves per samples in total). The Δ_{47} analyses of ostracod shells, which provide at the same time the $\delta^{18}O_{ost}$data, were carried out at the in the AMGC clumped isotope lab of the Vrije Universiteit Brussel (VUB), using a Nu Instruments Perspective-IS stable isotope ratio mass spectrometer (SIRMS) in conjunction with a Nu-Carb carbonate sample preparation system, as described in detail in De Vleeschouwer et al. (2022). The analyses were performed between March 2022 and November 2022. The carbonate standard ETH-4 was systematically measured and compared to InterCarb values (Bernasconi et al., 2021) to assess the accuracy and reproducibility. Analyses and results were monitored in the lab using the Easotope software (John and Bowen, 2016). Within the ClumpyCrunch software (Daëron, 2021), the raw measured Δ_{47} values were processed using the IUPAC Brand's isotopic parameters (Daëron et al., 2016) and converted to the ICDES 90 °C scale, using the most recent values for the ETH-1, ETH-2, and ETH-3 carbonate reference materials (Bernasconi et al., 2021). Analytical and calibration uncertainties were propagated to calculate the final uncertainties on temperatures. The Δ_{47} values were converted into temperatures using the unified calibration (Anderson et al., 2021) as suggested by Marchegiano et al. (2023) and the $\delta^{18}O_w$ values calculated from Δ_{47} and $\delta^{18}O_{ost}$ data using the formula of Kim and O'Neil (1997) for calcite (Table 1). Since the $\delta^{18}O_{ost}$ suffers a species-specific offset (Holmes and Chivas, 2002), to obtain meaningful comparisons, it is important to correct the

$\delta^{18}O_{ost}$ by removing the species-specific offset to normalize the $\delta^{18}O_{ost}$ values with the theoretical inorganic calcite deposited at the isotopic equilibrium at the same moment in the same environment. We used the values of these offsets previously calculated and reported for *C. angulata* (2.2‰, Von Grafenstein et al., 1999) and *C. torosa* (0.8‰ Keatings et al., 2007). The vital offset of *S. aculeata* and *H. salina* have never been calculated before and without the analyses of living shells these values cannot be validated. However, *E. mareotica* is considered to precipitate close to the isotopic equilibrium (Li and Liu, 2010) and because the lack of substantial difference between the $\delta^{18}O_{ost}$ values of *S. aculeata* and *E. mareotica* (0.009‰ in sample TRAH1–1 and TRAH1–2), we assume this is also the case for *S. aculeata* and *H. salina* (difference of 0.18 ‰ between TRA2 and TRA2B).

3. Results

3.1 Classic and clumped-isotopes

The Δ_{47} values of the ostracod samples range from 0.648 to 0.594 ‰ with a SE from 0.009 to 0.015 ‰ (Table 1). Values of the $\delta^{18}O_{ost}$ and $\delta^{13}C_{ost}$ vary from −0.45 ‰ to 3.20 ‰ and from −3.47 ‰ to 3.99 ‰ (SE of 0.1 ‰ on average). The number of replicated measurements carried out per sample is determined based on the availability of sample material. The large number of replicates per specimen ensures the robustness of the results. The repeatability along the 8 sessions of the standards used to standardize the results and the ostracod samples is 33.2 ppm and 31.4 ppm, respectively. The repeatability of the $\delta^{18}O_{ost}$ and $\delta^{13}C_{ost}$ is 39.0 ppm and 17.8 ppm, respectively. The ETH4 standard, used to assure and control the quality of the analyses, presents a Δ_{47} value of 0.446 ‰ and a standard error (SE) of 0.0059 for 67 replicates. The difference between our measured value of ETH4 and the official one from Bernasconi et al. (2021) (ETH4- Δ_{47}value of 0.4505 ± 0.0015) is negligible (Δ_{47} of 0.0045) and falls within the calculated SE. This confirms both the accuracy and precision of the Δ_{47} analyses presented in this study. The box plots for Δ_{47} temperatures (Fig. 6) are made including all replicate measurements per each sample (see Table 1 in supplementary material) and show median temperatures of 17 °C during the MIS3, of 12 °C during MIS2 and of 23 °C during the Holocene. The larger probability density in MIS3 and the Holocene is due to the internal higher replicate variability in the measured samples. This differs from the analytical uncertainties reported for each Δ_{47}-temperature data that is, instead, determined using the "pooled" standardization method outlined by Daëron (2021), which considers the reproducibility constraints obtained from both standard and sample analyses.

4. Discussion

4.1 Species-specific effect on the ostracod-Δ_{47} paleothermometer

In the first application of the ostracod-Δ_{47} thermometer on living ostracod that precipitated their shells at known temperatures, Marchegiano et al. (2023) demonstrated the absence of a vital offset at genus and species level. By converting the measured Δ_{47}values in temperatures, using the unified clumped isotope calibration of Anderson et al. (2021), ostracod species, coming from a lab culture (23 °C) and natural environments (12 and 4 °C) recorded the corresponding temperatures with a precision of around ± 2 °C (Marchegiano et al., 2023). Moreover, the species *E. virens* and *B. fuscata*that lived at the same time and environment and precipitated their shells at the same temperature, presents a very small offset of 0.5 °C that falls within the analytical uncertainty (Marchegiano et al., 2023).

To confirm the absence of a species-specific effect also in the fossil record, this study analyzed the Δ_{47} of two different ostracod species coming from the same sediment layers. *S. aculeata* (TRA-2) and *H. salina* (TRA2b) and *S. aculeata* (TRAH2–1) and *E. mareotica* (TRAH2–2) were abundantly found in the same ostracod assemblages (Marchegiano et al., 2018 and 2019) and modern studies suggest that they all live during the warm season (Meish, 2000 and Li and Liu, 2010). We can thus assume that they precipitated their shells at the same time, season and in the same temperature and environment. This is also supported by $\delta^{18}O_c$ and $\delta^{13}C_c$ analyses performed on ostracod shells, which show comparable values and thus similar livelihood in the same sediment layers (*S. aculeata* (TRA-2) $\delta^{18}O_c$ 0.03‰ and $\delta^{13}C_c$ 3.99‰ and *H. salina* (TRA2b) $\delta^{18}O_c$−0.21‰ and $\delta^{13}C_c$ 3.6‰; *S. aculeata* (TRAH2–1) $\delta^{18}O_c$ 0.61‰ and $\delta^{13}C_c$ 3.58‰ and *E. mareotica* (TRAH2–2) $\delta^{18}O_c$ 0.69‰ and $\delta^{13}C_c$ 1.7‰).

The absence of a consistent offset, within the analytical uncertainty, between *S. aculeata*(TRA-2) and *H. salina* (TRA2b) (Δ_{47} 0.002 ± 0.01‰, Table1) and between *S. aculeata*(TRAH2–1) and *E. mareotica* (TRAH2–2) (Δ_{47} 0.001 ± 0.01‰ Table1) confirms the absence of the vital offset in fossil ostracod shells at genus and species level. This finding is also supported by the analyses of recent shells of *C. torosa* (TRAR2, 22.5 ± 2.3 °C today average warm season T is of 21.4 °C) and *C. angulata* (TRAR2 8 ± 2.9 °C, today average cold season T is of 9.5 °C) both recording temperature very close to the ones measured today at lake Trasimeno during the respective precipitation season.

Although there is no vital offset in the ostracod-Δ_{47} signal, it remains important to know the timing of precipitation of ostracod shells to provide accurate paleotemperaturereconstructions. Therefore, not all species can be mixed for Δ_{47} analyses but only the ones that precipitate their shells during the same season. Thus, by combining the Δ_{47}technique, with paleontological and biological knowledge of the ostracod fauna, the ostracod-Δ_{47} paleothermometer has the potential to accurately reconstruct past temperatures and seasonality variations.

4.2 Ostracod-Δ_{47} temperature reconstruction

To correctly use ostracod shells as a geochemical tool, it is necessary to understand their ecological preferences and life history (i.e., timing of shell precipitation). The species used in this study are widespread and quite well known. *Cyprideis torosa* (Fig. 4) lives at a wide range of salinities (Griffith and Holmes, 2000) in permanent water conditions (Meisch, 2000) and occurs today in the freshwater Lake Trasimeno (Marchegiano et al., 2017). This species seems to produce two generations per year with adulthood calcification in spring and autumn (Heip, 1976 and Roberts et al., 2020). Today, the water temperature of Lake Trasimeno ranges from 11 °C (April) to 23 °C (June) during spring and from 16 °C (October) to 8 °C (December) in autumn (World Lake Database, 2013). The Δ_{47} analyses obtained on recent *C. torosa* shells (TRAR2) yield temperatures of 22.5 ± 2.3 °C. Therefore, it seems that at Lake Trasimeno, there is a prevalence of spring generations or that shells continue to calcify also during the summer. This work considers *C. torosa* species as indicative of late-spring/early-autumn (warm season) temperatures (today May–October water mean T are 21.4 °C). In the Trasimeno record, *C. torosa* is very abundant during the relatively warm and humid MIS 3 (from ca. 46 to 34 cal ky BP), and the Holocene, indicating a permanent lake with low saline water (Marchegiano et al., 2018 and 2019). The *C. torosa* Δ_{47} temperature during MIS 3 ranges from 15 ± 1.6 °C to 22 ± 2.3 °C and of 23.2 ± 2.5 °C in the Early Holocene (Table 2). *Sarcypridopsis aculeata* and *Eucypris mareotica* (Fig. 4) are often found together and indicate ephemeral-shallow lake conditions and high salinity conditions (Martin-Puertas et al., 2008). They do not live in Lake Trasimeno today (Marchegiano et al., 2017) and disappeared from the fossil record at the Pleistocene-Holocene transition suggesting a change from prevalent ephemeral to permanent lake conditions (Marchegiano et al., 2018 and 2019). S. aculeata develops up to three summer generations per year (time of shells calcification) and adults very rarely survive in the colder months (Meish, 2000). E. mareotica hatches between late June and early July and reaches the adults stage in late July-early August (Li and Liu, 2010). Today, the water temperature of Lake Trasimeno during summer ranges from 26 °C (August) to 21 °C (September) (World Lake database 2023) (Table 2). Because these species are not part of the living fauna today, Δ_{47} analyses on recent S. aculeata and E. mareotica are not possible to confirm their precipitation season in Lake Trasimeno. However, assuming that during the entire Holocene temperatures were similar to today, the Δ_{47} analyses made on Early Holocene S. aculeatashells (TRA2, temperature of 24.9 ± 2 °C), confirm that S. aculeata precipitates its shell during the summer season at Lake Trasimeno (today mean water T are of 24 °C). The seasonal attribution can also be extended to E. mareotica since no significant difference in temperature is observed between samples TRAH2–1 (S. aculeata) and TRAH2–2 (E. mareotica) (13 and 13.2 ± 3 °C respectively) originating from the same sediment layers. In the Trasimeno record, S. aculeata and E. mareotica form the most abundant species at the end of the MIS 3 and during the cold and dry MIS 2 (from ca. 34 to 10 ky BP) indicating shallow-ephemeral lake conditions and higher salinities (Marchegiano et al., 2018). The Δ_{47} temperatures derived from S. aculeata shells during MIS2 range from 10 ± 2.9 °C to 17 ± 3.1 °C and it is of 24.9 ± 2 °C at the Pleistocene-Holocene transition (Table 2).

Heterocypris salina (Fig. 4) is a cosmopolitan species often found together with S. aculeataand C. torosa but it does not tolerate ephemeral conditions. This species lives today in Lake Trasimeno (Marchegiano et al., 2017). It has 2 to 3 summer generations (time of shells calcification) and lives for 45 days (Meish, 2000). At the Pleistocene-Holocene transition, samples TRA 2 and TRA 2B, *S. aculeata* and *H. salina* are measured and provide a very similar temperature (24.9 ± 2 °C and 24.3 ± 2.2 °C respectively) confirming that they both precipitate during the summer season (Fig. 5 and Table 2).

Candona angulata (Fig. 4) prefers slightly salty permanent waters and is often found together with *H. salina* and C. torosa. Today, this species lives in the deepest part of Lake Trasimeno in association with *C. torosa* (Marchegiano et al., 2017). *C. angulata* is a winter species that lives from November to March and precipitates its shell from November to February (Meish, 2000). Today, the winter water temperatures at Lake Trasimeno range from 12 °C (November) to 7 °C (February) (World Lake Database, 2013). In the Trasimeno record, C. angulata is present almost during the entire interval, but it is found at such small percentages that Δ_{47} analyses could not be conducted. It is, instead, very abundant in the Holocene and in this study is used to reconstruct seasonal variations during this time period. The Δ_{47} analyses made on C. angulata (TRAR2) gave temperatures of 8 ± 2.9 °C in recent shells and of 11.8 ± 2.1 °C in the Early Holocene (TRAHOL1) (Fig. 5 and Table 2). On the same samples *C. torosa*, a late-spring/early-autumn species, records temperatures of 22.5 ± 2.3 °C and 23.2 ± 2.5 °C respectively (Fig. 5). The good correspondence with today mean water temperatures of Lake Trasimeno (8 °C during November-February and of 21.4 °C during May-October) confirms the accuracy of the analyses, the applicability of the ostracod-Δ_{47} on fossil shells and the ability of the method to reconstruct paleotemperatures, even at seasonal scale.

4.3. Paleoclimate reconstruction

In this study, all Δ_{47} temperatures measured on *C. torosa, S. aculeata, E. mareotica,* and *H. salina* shells are considered as warm season temperatures (from late spring to early autumn). Instead, Δ_{47} temperatures from *C. angulata* are considered as cold season temperatures (from November to March). Changes in shell calcification season along the Trasimeno record are unlikely because drastic hydrological variations only occurred at the transition between the MIS3 and 2 and MIS2 and the Holocene. Within each interval, where the same ostracod species are used for Δ_{47} temperatures reconstruction, lake level and water geochemistry do not show large variations as supported by ostracod assemblages, sedimentology, and geochemical analyses (Marchegiano et al., 2018 and Francke et al., 2022). Also, during periods colder than today, if a change in shell calcification season had happened, it would usually have occurred toward warmer temperatures (seasons) (Yue et al., 2022 and Van der Meeren et al., 2011). Temperature changes during the analyzed interval are not biased by change in shell precipitation season.

In a previous study (Marchegiano et al., 2020), the Mutual Ostracod Temperature Range transfer function (MOTR, Horne, 2007) was applied to all the samples from 7.4 to 3.1 m depth of the Trasimeno core. The MOTR method uses temperature ranges of species that have been calibrated by correlating their distributions using DIVA-GIS software (version 7.5) and comparing them with the air temperatures of the WorldClim database (version 1.3) (Hijmans et al., 2001). Past mean January (coldest month) and July (warmest month) air temperature ranges for specific ostracod assemblages are reconstructed by overlapping the calibrated temperature ranges of each species found in the given assemblage (Mutual Climate Range principle, Atkinson et al., 1986).

Warm season water temperatures based on ostracod-Δ_{47} fall within the uncertainties into the July minimum and maximum mutual ostracod air temperature range (MOTR) reconstructed for this interval (Marchegiano et al., 2020), and correspond well to the peak (higher T) and minima (lower T) of the MOTR curves (Fig. 5). This correspondence suggests a close connection between air and water temperature variations in Lake Trasimeno and a prompt reaction of the lake system to climatic changes. The LATEMIS3 (Table 1) is the only sample, including the Δ_{47} uncertainties that falls outside the MOTR (Fig. 5). This could be explained by a lack of (or reduced) response of the ostracod fauna (i.e., change in the ostracod assemblages) to the fast environmental change at the onset of this cold event (probably associated to H3).

Colder and warmer periods at Lake Trasimeno are certainly linked to the millennial-scale climatic variations (warm-humid interstadial GI, cold-arid stadial GS and coldest and driest Heinrich events), as confirmed by prior studies (Marchegiano et al., 2018, 2020 and Francke et al., 2022). These millennial-scale climatic events are likely associated to reduction (cold events) and enhancing (warm events) of the Atlantic Meridional Overturning Circulation (AMOC) plus a displacement of cooling conditions throughout the central Mediterranean area during the GS and Heinrich events (Francke et al., 2022). However, because of chronological limitations, it is not possible to identify exactly which events have been recorded.

The *C. torosa*-Δ_{47} temperatures during MIS3 ranges from 15 ± 1.6 °C to 22 ± 2.3 °C, with a median temperature of 17 °C, indicating warm season temperatures from 2 to 6 °C lower than today (Fig. 6 and Table 2). During the same interval, air temperatures of the coldest month based on pollen from south Italy (Lake Monticchio) fall around −8 °C, reaching −16 °C in the coldest events (Allen et al., 1999). Meanwhile, marine annual surface temperatures based on alkenones for the Alboran Sea range from 10 to 16 °C (Cacho et al., 1999) (Fig. 6). In this interval, the coldest event (15 ± 1.6 °C) at Lake Trasimenno can be tentatively associated to the Heinrich events (H4). Likewise, the warmest events (20 ± 2.1 and 22 ± 2.3 °C) are likely linked to the GIs (10 and 8) and the event at ca. 18 ± 1.7 °C to is probably associated with the GS (12).

At the transition between MIS 3 and MIS 2, which corresponds to the onset of full glacial conditions, *S. aculeata*-Δ_{47} warm season temperature drastically decrease to 10 ± 2.9 °C and then slowly increase up to 15 ± 3 °C at the end of MIS 2. The median warm season temperature for the MIS2 is 12 °C (from 12 to 7 °C colder than today warm season mean temperatures) (Fig. 6). The substantial decrease in temperature observed at Lake Trasimeno is only marginally reflected in the marine surface mean annual temperatures at the Alboran Sea and it is nearly absent in the Monticchio winter temperature, which remains around −8 °C. This divergence in behavior between the three records may be attributed to a diverse climate response and/or the influence of regional parameters. However, differences between the air temperature of the coldest month (pollen from Lake Monticchio, southern Italy) and warm season water temperatures (Δ_{47} – ostracod from Lake Trasimeno, central Italy) can potentially be explained by the reduced summer insolation experienced during MIS2 (Fig. 6). The coldest temperatures in this interval can be tentatively associated to the Heinrich's events. Considering the last cold event of this interval was the Younger Dryas, summer temperatures at Lake Trasimeno (15 ± 3 °C) match the pollen summer temperature at Lake Matese (southern Italy, Robles et al., 2023) and the chironomid summer temperatures at Lake Piccolo di Avigliana (northern Italy, Larocque and Finsinger, 2008), both recording a temperature of 16 °C. The brGDGT mean annual temperatures of Lake Matese, in the same period, is instead 12 °C (Robles et al., 2023) (Fig. 6).

At the Pleistocene - Holocene transition (i.e., the onset of the interglacial), warmer season temperatures increased by 10 °C (temperatures of 25 ± 2 °C, 3 °C higher than the warmer season temperatures today, see Table 2) with Holocene median temperatures of 23 °C (Fig. 6). Because of the very shallow/ephemeral conditions of Lake Trasimeno during MIS 2 and the Pleistocene – Holocene transition (Marchegiano et al., 2018 and 2019), a possible overestimation of lake water temperatures from 2 to 4 °C (i.e., the modern temperature difference between lake water and atmosphere at Lake Trasimeno today) need to be considered as temperatures could be closer to the atmospheric ones.

During the Early Holocene, the warm season temperatures closely resemble those of the present day. However, the cold season temperature (12 ± 2.1 °C) is approximately 4 °C warmer than today (8 °C), indicating a reduced seasonality (Fig. 6). This decrease in seasonality during the Early Holocene aligns well with previous findings in hydrological records from central-southern Italy (Magny et al., 2012 and Marchegiano et al., 2019). The temperature record based on Δ_{47} measurements from Lake Trasimeno provides the first confirmation of a lower seasonality, also in temperatures, than today for central-southern Italy. Latest Holocene (last ca. 1 ky) Δ_{47} temperatures are the same as today at Lake Trasimeno (8 °C winter and 22 °C for late spring/early autumn).

4.4 Paleohydrology reconstruction

Because of the endorheic and shallow nature of Lake Trasimeno, its water geochemistry strictly depends on the climatic variations and particularly, on the E/P (Frondini et al., 2019). This was confirmed by the comparison between recent $\delta^{18}O$ and $\delta^{2}H$ lake water values and the local evaporation line (LEL) (Frondini et al., 2019) and by the moderate positive correlation ($R^2 = 0.24$) between past $\delta^{13}C$ and $\delta^{18}O$ in bulk carbonates data indicating an exchange between lake water and atmosphere due to evaporation (Francke et al., 2022). The oxygen isotopic composition of precipitation ($\delta^{18}O_p$) at Lake Trasimeno today varies between −9.9‰ in January and −1.9‰ in July (Bowen and Wilkinson, 2002) as a consequence of decreasing summer precipitation and increasing temperatures. The differences between $\delta^{18}O_p$ and $\delta^{18}O_w$ today is between ca. 9 and 11 ‰ during winter and ca. 3 and 6 ‰ during summer, indicating a large loss of light isotope ($\delta^{16}O$) through evaporation. However, the small difference of 2 ‰ between today $\delta^{18}O_w$summer (ca. 3.8 to 1.2 ‰) and $\delta^{18}O_w$ winter (−1 to 1

‰) (monitored values from Frondini et al., 2019) also suggests a minor contribution of summer precipitation to the annual $\delta^{18}O_w$ budget.

There is a good agreement between the $\delta^{18}O_w$ values reconstructed from ostracod shells and the $\delta^{18}O$ curve on bulk carbonate from Francke et al. (2022) suggesting a co-variance of these two isotopic signals (Fig. 5). However, the slight difference in the absolute values between $\delta^{18}O$ of calcite (measured on bulk carbonate) and $\delta^{18}O_w$ of the water (measured on ostracods) can be due to both the isotopic fractionation between $\delta^{18}O$ of the water and the one recorded in the carbonate as well as a difference in timing of carbonate precipitation between ostracod (few hours and related to the calcification season) and bulk carbonate (annual average).

During the mild and more humid MIS 3, $\delta^{18}O_w$ warm season values range from 2.0 ± 0.2 to 1.0 ± 0.2 ‰, within the present-day variability. Lower values correspond to colder temperatures (18 ± 1.7 °C) and higher values to warmer ones (ca. 22 ± 2.3 °C) suggesting colder-dryer and warmer-humid periods. Although ostracod assemblages indicate permanent lake conditions, they also suggest that the variations in precipitation and/or evaporation amount remain low. The lack of abrupt and extreme hydrologicalfluctuations, which are evident in the NGRIP record (Rasmussen et al., 2016) during the MIS 3, in favor of a gradual decline in rainfall, and thus of the lake level, from the MIS 3 to MIS 2, has also been identified in speleothem records from southern and central Italy (Columbo et al. 2020). This pattern appears associated with a shift in the moisture source from the Atlantic, which was the primary source during the MIS 4 and 5, to the Mediterranean, attributed to the expansion of the northern ice sheets, combined with the decreased effectiveness of the westerlies in delivering moisture (i.e., less moisture availability in the Mediterranean) (Columbu et al., 2020).

During the cold and arid MIS2, $\delta^{18}O_w$ warm season values range from 1.5 ± 0.3 to 0 ± 0.3 ‰ (Fig. 5). Considering that several studies in central and southern Italy, including pollen (e.g., Allen et al., 1999; Follieri et al., 1988) and speleothem records (Columbo et al., 2022), suggest a low precipitation during MIS2 in the central Mediterranean area, and that ostracod assemblages at Lake Trasimeno also indicate low lake level/ephemeral conditions (Marchegiano et al., 2018), the lighter values, in average, during MIS2 compared to MIS3 can be due to a decrease of evaporation as consequence of lower summer insolation (Fig. 5). A trend toward heavier $\delta^{18}O_w$ values, from around 28 ky to ca. 16 ky indicating a general decrease of rainfall amount (Fig. 5), corresponds well to the $\delta^{18}O_c$ speleothem records from Sant'Angelo cave (southern Italy, Columbo et al., 2022), Ostolo cave (Northern Iberian Peninsula, Bernal-Wollum et al., 2021) and Soreq cave (Israel, Bar-Matthews et al., 2003). This trend, also observed in the NGRIP record (Rasmussen et al., 2016), confirms the continues influence of the ice-sheet extent variations at higher latitude on central Mediterranean area. The datapoint likely associated to the Younger Dryas event (Fig. 4 and 5) at Lake Trasimeno (ca. 12.5ky), shows warmer season $\delta^{18}O_w$ lighter values ($\delta^{18}O_w$ 0.6 ± 0.3 ‰). This anomaly, compared to other speleothem records in southern Italy, which present mean annual heavier $\delta^{18}O_c$values associated to dryer conditions, can be explained by cold and wetter summers and cold and dryer winters. This seasonal variation in rainfall amount have been also recognized in northern Iberia speleothems (Baldini et al., 2019 and Bernal-Wormull et al., 2023).

At the Pleistocene – Holocene transition, $\delta^{18}O_w$ warmer season values are the highest of the entire interval ($\delta^{18}O_w$ 2.7 ± 0.2 ‰) probably due to an increase in evaporation (water enriched of heavier $\delta^{18}O$) caused by high temperatures and highest summer insolation (Fig. 5). Ostracod assemblages still indicate low lake level/ephemeral conditions (Marchegiano et al., 2018) suggesting warmer season conditions more arid than today, as also recorded by pollen archives from southern and central Italy (Magny et al., 2012). On the contrary, speleothem $\delta^{18}O_c$ mean annual records, indicate the onset of wetter conditions due to the decrease of ice-sheet extent, high availability of Atlantic moisture and increase of westerly-driven winter rainfall amount across the Mediterranean (Columbo et al., 2022). This contrasting signal continues to support a different seasonal rainfall amount most probably linked to summer insolation.

In the Early Holocene, $\delta^{18}O_w$ decrease and warm and cold season values are very close ($\delta^{18}O_w$ 1 ± 0.2 and 0.9 ± 0.2 ‰) (Fig. 5). Ostracod assemblages indicate an increase of lake level (Marchegiano et al., 2019), these values suggest lower E/P ratios (and thus high humidity) during both seasons, documenting/supporting low seasonality contrast in the hydrology. However, seasonal temperatures are different (11.8 ± 2.1 and 23.2 ± 2.5 °C). The same paleohydrological behavior has been observed in Lake Pergusa and Lake Preola (southern Italy) (Magny et al., 2012) and in Sant'Angelo cave (southern Italy, Columbo et al., 2022), as well as in eastern Mediterranean (Marino et al., 2009; Develle et al., 2010). Conversely, records from northern Italy and western Mediterranean present a higher seasonality contrast with drier summers during and after ca. 9800 cal a BP (Finsinger et al., 2010 and Peyron et al., 2011). This study also confirms Early Holocene, climatic conditions in central Italy similar to those ones in southern Italy. Therefore, the climatic limit between northern and southern climatic zone in Italy, previously settled at 40° latitude by Magny et al. (2012), needs to be moved to 43° latitude, as previously suggested by Marchegiano et al. (2019).

In the latest part of the Holocene, the reconstructed $\delta^{18}O_w$ values (Fig. 5) appear similar to today and indicate a difference of 2‰ between seasons suggesting high winter and low summer precipitation as typical of present-day central Mediterranean climate. This larger contrast of precipitation amount between seasons seems to have started in central – southern Italy around ca. 4.5 cal ky BP (Magny et al., 2012). Similar seasonal patterns in precipitations have been also observed in the western Mediterranean (García-Alix et al., 2021; Toney et al., 2020).

5. CONCLUSIONS

The analyses carried out on recent samples (last ca. 1ky) confirm the applicability of the ostracod-clumped isotope thermometer to reconstruct paleotemperatures, seasonalityand hydrological conditions. The absence of a vital effect at genus and species level is confirmed also in the signal of fossil Δ_{47}-ostracod shells. However, despite the lack of a vital effect, in environments with seasonal temperature variations, not all species can be measured together. Only species that precipitate their shell during the same season can be combined.

The application of the ostracod-Δ_{47} thermometer on the Trasimeno lacustrine core (central Italy), provides the very first absolute continental warm season paleotemperature and hydrological conditions for the last 43 ky in the central Mediterranean area. It indicates warm season temperatures heavily impacted by millennial scale climatic events. Insolation conditions enhance the effect of the millennial scale climate variability, by increasing warm season temperature differences between warmer/high insolation MIS 3 (median temperatures of 17 °C), colder/lower insolation MIS2 (median temperatures of 12 °C) and warmer/higher insolation during Holocene (median temperatures of 23 °C). This trend is also observed in warm season hydrological conditions with high evaporation during MIS3 and Holocene and low ones in the MIS2.

During the Early Holocene, cold season temperatures appear warmer than today, and similar hydrological conditions exist between warm and cold seasons underlying a lower seasonality contrast than today with enhanced warm season precipitation.

The new Δ_{47}-ostracod thermometer represents a major advance to better document past climate seasonal fluctuations, especially on the continents, as these organisms are common in many lacustrine setting.

DECLARATION OF COMPETING INTEREST

The authors declare that they have no known competing financial interests or personal relationships that could have appeared to influence the work reported in this paper.

AKNOWLEDGMENTS

We thank the AMGC-VUB lab manager David Verstraeten for his immeasurable help and support during the analyses, as well as David De Vleeschower and Jose Manuel Mesa-Fernández for the helpful discussions. The study was in part funded by Junta de Andalucía-Consejería de Universidad, Investigación e Innovación-Proyecto 21.00020. MM wish to express their thanks for the financial support of the Swiss National Science Foundation (P2GEP2_181063). PC, SG. and CS thank the Research Foundation Flanders for funding the IRMS acquisition and the VUB Strategic Research for support.

DATA AVAILABILITY

Data are available in the supplementary material section during the review process, and they will be successively deposited in a data repository, most probably EarthChem.

REFERENCES

Abrantes, F., Voelker, A. (Helga L., Sierro, F.J., Naughton, F., Rodrigues, T., Cacho, I., Ariztegui, D., Brayshaw, D., Sicre, M.-A., Batista, L., 2012. Paleoclimate Variability in the Mediterranean Region, in: The Climate of the Mediterranean Region. Elsevier, pp. 1–86. https://doi.org/10.1016/B978-0-12-416042-2.00001-X

Ali, E., W. Cramer, J. Carnicer, E. Georgopoulou, N.J.M. Hilmi, G. Le Cozannet, and P. Lionello, 2022: Cross-Chapter Paper 4: Mediterranean Region. In: *Climate Change 2022: Impacts, Adaptation, and Vulnerability.* Contribution of Working Group II to the Sixth

Assessment Report of the Intergovernmental Panel on Climate Change [H.-O. Pörtner, D.C. Roberts, M. Tignor, E.S. Poloczanska, K. Mintenbeck, A. Alegría, M. Craig, S. Langsdorf, S. Löschke, V. Möller, A. Okem, B. Rama (eds.)]. Cambridge University Press, Cambridge, UK and New York, NY, USA, pp. 2233-2272, doi:10.1017/9781009325844.021

Allen, J.R.M., Brandt, U., Brauer, A., Hubberten, H.-W., Huntley, B., Keller, J., Kraml, M., Mackensen, A., Mingram, J., Negendank, J.F.W., Nowaczyk, N.R., Oberhänsli, H., Watts, W.A., Wulf, S., Zolitschka, B., 1999. Rapid environmental changes in southern Europe during the last glacial period. Nature 400, 740–743. https://doi.org/10.1038/23432

Anderson, N., Kelson, J.R., Kele, S., Daëron, M., Bonifacie, M., Horita, J., Mackey, T.J., John, C.M., Kluge, T., Petschnig, P., Jost, A.B., Huntington, K.W., Bernasconi, S.M., Bergmann, K.D., 2021. A unified clumped isotope thermometer calibration (0.5-1100C) using carbonate-based standardization (preprint). Geochemistry. https://doi.org/10.1002/essoar.10505702.1

Atkinson, T. C., Briffa, K. R., Coope, G. R., Joachim, M. J. & Perzy, D. W. 1986: Climatic calibration of coleopteran data. In Berglund, B. E. (ed.): Handbook of Holocene Palaeoecology and Palaeohydrology, 851–858. Wiley, New York.

Baldini, L.M., Baldini, J.U.L., McDermott, F., Arias, P., Cueto, M., Fairchild, I.J., Hoffmann, D.L., Mattey, D.P., Müller, W., Nita, D.C., Ontanon, R., Garcia- Monco, C., Richards, D.A., 2019. North Iberian temperature and rainfall sea- sonality over the younger Dryas and Holocene. Quat. Sci. Rev. 226, 105998. https://doi.org/10.1016/j.quascirev.2019.105998.

Bar-Matthews, M., Ayalon, A., Gilmour, M., Matthews, A. & Hawkesworth, C. J., 2003. Sea–land oxygen isotopic relationships from planktonic foraminifera and speleothems in the

Eastern Mediterranean region and their implication for paleorainfall during interglacial intervals. Geochimica et Cosmochimica Acta 67, 3181–3199.

Bernal-Wormull, J. L., Moreno, A., Perez-Mejias, C., Bartolome, M., Aranburu, A., Arriolabengoa, E., Cacho, I., Spotl, C., Edwars, R.L., Cheng, H., 2021. Immediate temperature response in northern Iberia to last deglacial changes in the North Atlantic. *Geology* no. **49**, 999–1003.

Bernal-Wormull, J. L., Moreno, A., Bartolome, M., Arriolabengoa, M., Perez-Mejias, C., Iriarte, E., Osacar, C., Spotl, C., Sroll, H., Cacho, I., Edwars, R.L., Cheng, H., 2023. New insight into climate of northern Iberia during the Younger Dryas and Holocene: The Mendukilo multi-speleothem record. Quaternary research review, 305. https://doi.org/10.1016/j.quascirev.2023.108006

Bernasconi, S.M., Daëron, M., Bergmann, K.D., Bonifacie, M., Meckler, A.N., Affek, H.P., Anderson, N., Bajnai, D., Barkan, E., Beverly, E., Blamart, D., Burgener, L., Calmels, D., Chaduteau, C., Clog, M., Davidheiser-Kroll, B., Davies, A., Dux, F., Eiler, J., Elliott, B., Fetrow, A.C., Fiebig, J., Goldberg, S., Hermoso, M., Huntington, K.W., Hyland, E., Ingalls, M., Jaggi, M., John, C.M., Jost, A.B., Katz, S., Kelson, J., Kluge, T., Kocken, I.J., Laskar, A., Leutert, T.J., Liang, D., Lucarelli, J., Mackey, T.J., Mangenot, X., Meinicke, N., Modestou, S.E., Müller, I.A., Murray, S., Neary, A., Packard, N., Passey, B.H., Pelletier, E., Petersen, S., Piasecki, A., Schauer, A., Snell, K.E., Swart, P.K., Tripati, A., Upadhyay, D., Vennemann, T., Winkelstern, I., Yarian, D., Yoshida, N., Zhang, N., Ziegler, M., 2021. InterCarb: A Community Effort to Improve Interlaboratory Standardization of the Carbonate Clumped Isotope Thermometer Using Carbonate Standards. Geochem Geophys Geosyst 22. https://doi.org/10.1029/2020GC009588

Blaauw, M., Christen, J.A., 2011. Flexible paleoclimate age-depth models using an autoregressive gamma process. Bayesian Anal. 6. https://doi.org/10.1214/11-BA618

Blaauw, M., Christen, J.A., Bennett, K.D., Reimer, P.J., 2018. Double the dates and go for Bayes — Impacts of model choice, dating density and quality on chronologies. Quaternary Science Reviews 188, 58–66. https://doi.org/10.1016/j.quascirev.2018.03.032

Börner, N., De Baere, B., Yang, Q., Jochum, K.P., Frenzel, P., Andreae, M.O., Schwalb, A., 2013. Ostracod shell chemistry as proxy for paleoenvironmental change. Quaternary International 313–314, 17–37. https://doi.org/10.1016/j.quaint.2013.09.041

Cacho, I., Grimalt, J.O., Pelejero, C., Canals, M., Sierro, F.J., Flores, J.A., Shackleton, N., 1999. Dansgaard-Oeschger and Heinrich event imprints in Alboran Sea paleotemperatures. Paleoceanography 14, 698–705. https://doi.org/10.1029/1999PA900044

Chivas, A.R., De Deckker, P., Shelley, J.M.G., 1983. Magnesium, strontium and barium partitioning in non marine ostracod shells and their use in paleoenvironment reconstructions – a preliminary study., in: Applications of Ostracoda. University of Houston, TX, pp. 238–249.

Columbu, A., Chiarini, V., Spotl, C., Benazzi, S., Hellstrom, J., Cheng, H., De Waele, 2020. Speleothem record attests to stable environmental conditions during Neanderthal-Modern Human turnover in Southern Italy. Nature Ecology Evolution 4, 1188–1195, 37. Zielhofer, C. et al. Atlantic forcing of Weste

Columbo, A., Spotl, C., Fohlmeister, J., Hsun-Ming, H., Chiarini, V., Hellstrom, J., Cheng, H., Shen, C., De Waele, J., 2022. Central Mediterranean rainfall varied with high northern latitude temperatures during the las deglaciation. Communications earth & environment 3, 181. https://doi.org/10.1038/s43247-022-00509-3

Daëron, M., 2021. Full Propagation of Analytical Uncertainties in Δ_{47} Measurements. Geochem Geophys Geosyst 22. https://doi.org/10.1029/2020GC009592

Daëron, M., Blamart, D., Peral, M., Affek, H.P., 2016. Absolute isotopic abundance ratios and the accuracy of Δ47 measurements. Chemical Geology 442, 83–96. https://doi.org/10.1016/j.chemgeo.2016.08.014

Develle AL, Herreros J, Vidal L, et al. 2010. Controlling factors on a palaeo-lake oxygen isotope record (Yammo ¨uneh, Lebanon) since the Last Glacial Maximum. Quaternary Science Reviews 29: 865886.

De Vleeschouwer, D., Peral, M., Marchegiano, M., Füllberg, A., Meinicke, N., Pälike, H., Auer, G., Petrick, B., Snoeck, C., Goderis, S., Claeys, P., 2022. Plio-Pleistocene Perth Basin water temperatures and Leeuwin Current dynamics (Indian Ocean) derived from oxygen and clumped-isotope paleothermometry. Clim. Past 18, 1231–1253. https://doi.org/10.5194/cp-18-1231-2022

de Winter, N.J., Müller, I.A., Kocken, I.J., Thibault, N., Ullmann, C.V., Farnsworth, A., Lunt, D.J., Claeys, P., Ziegler, M., 2021. Absolute seasonal temperature estimates from clumped isotopes in bivalve shells suggest warm and variable greenhouse climate. Commun Earth Environ 2, 121. https://doi.org/10.1038/s43247-021-00193-9

Eiler, J.M., 2007. “Clumped-isotope” geochemistry—The study of naturally-occurring, multiply-substituted isotopologues. Earth and Planetary Science Letters 262, 309–327. https://doi.org/10.1016/j.epsl.2007.08.020

Finsinger W, Colombaroli D, de Beaulieu JL, et al. 2010. Early to midHolocene climate change at Lago dell’Accesa (central Italy): climate signal or anthropogenic bias? Journal of Quaternary Science 25: 1239–1247.

Follieri, M., Magri, D., Sadori, L., 1988. 250’000-year pollen record from Valle di Castiglione (Roma). Pollen et Spore 33, 329–356.

Francke, A., Lacey, J.H., Marchegiano, M., Wagner, B., Ariztegui, D., Zanchetta, G., Kusch, S., Ufer, K., Baneschi, I., Knödgen, K., 2022. Last Glacial central Mediterranean hydrology inferred from Lake Trasimeno's (Italy) calcium carbonate geochemistry. Boreas bor.12552. https://doi.org/10.1111/bor.12552

Frondini, Dragoni, Morgantini, Donnini, Cardellini, Caliro, Melillo, Chiodini, 2019. An Endorheic Lake in a Changing Climate: Geochemical Investigations at Lake Trasimeno (Italy). Water 11, 1319. https://doi.org/10.3390/w11071319

García-Alix, A., Camuera, J., Ramos-Román, M.J., Toney, J.L., Sachse, D., Schefuß, E., Jiménez-Moreno, G., Jiménez-Espejo, F.J., López-Avilés, A., Anderson, R.S., Yanes, Y., 2021. Paleohydrological dynamics in the Western Mediterranean during the last glacial cycle. Global and Planetary Change 202, 103527. https://doi.org/10.1016/j.gloplacha.2021.103527

Gasperini, L., Barchi, M.R., Bellucci, L.G., Bortoluzzi, G., Ligi, M., Pauselli, C., 2010. Tectonostratigraphy of Lake Trasimeno (Italy) and the geological evolution of the Northern Apennines. Tectonophysics 492, 164–174. https://doi.org/10.1016/j.tecto.2010.06.010

Gasperini, L., Peteet, D., Bonatti, E., Gambini, E., Polonia, A., Nichols, J., Heusser, L., 2022. Late Glacial and Holocene environmental variability, Lago Trasimeno, Italy. Quaternary International 622, 21–35. https://doi.org/10.1016/j.quaint.2021.10.011

Gornitz, V. (Ed.), 2009. Encyclopedia of paleoclimatology and ancient environments, Encyclopedia of earth sciences series. Springer, Dordrecht, Netherlands ; New York.

Grafenstein, U. von, Erlenkeuser, H., Brauer, A., Jouzel, J., Johnsen, S.J., 1999. A Mid-European Decadal Isotope-Climate Record from 15,500 to 5000 Years B.P. Science 284, 1654–1657. https://doi.org/10.1126/science.284.5420.1654

Griffiths, H.I. and Holmes, J.A., 2000. Non-marine ostracods and Quaternary palaeoenvironments. Quaternary Research Association Technical Guide 8, 179.

Heiri, O., Ilyashuk, B., Millet, L., Samartin, S., Lotter, A.F., 2015. Stacking of discontinuous regional palaeoclimate records: Chironomid-based summer temperatures from the Alpine region. The Holocene 25, 137–149. https://doi.org/10.1177/0959683614556382

Heip, C., 1976, The life-cycle of Cyprideis torosa (Crustacea, Ostracoda): Oecologia, v. 24, p. 229–245.

Hijmans, R. J., Guarino, L., Cruz, M. & Rojas, E. 2001: Computer tools for spatial analysis of plant genetic resources data: 1 DIVA GIS. Plant Genetic Resources Newsletter 127, 15–19.

Holmes, J.A., Chivas, A.R., 2002. Ostracod shell chemistry — overview, in: Holmes, J.A., Chivas, A.R. (Eds.), Geophysical Monograph Series. American Geophysical Union, Washington, D. C., pp. 185–204. https://doi.org/10.1029/131GM10

Holmes, J.A., De Deckker, P., 2012. The Chemical Composition of Ostracod Shells, in: Developments in Quaternary Sciences. Elsevier, pp. 131–143. https://doi.org/10.1016/B978-0-444-53636-5.00008-1

Horne, D.J., 2007. A Mutual Temperature Range method for Quaternary palaeoclimatic analysis using European nonmarine Ostracoda. Quaternary Science Reviews 26, 1398–1415. https://doi.org/10.1016/j.quascirev.2007.03.006

John, C.M., Bowen, D., 2016. Community software for challenging isotope analysis: First applications of ‘Easotope’ to clumped isotopes: Community software for challenging isotope analysis. Rapid Commun. Mass Spectrom. 30, 2285–2300. https://doi.org/10.1002/rcm.7720

Keatings, K.W., Hawkes, I., Holmes, J.A., Flower, R.J., Leng, M.J., Abu-Zied, R.H., Lord, A.R., 2007. Evaluation of ostracod-based palaeoenvironmental reconstruction with instrumental data from the arid Faiyum Depression, Egypt. J Paleolimnol 38, 261–283. https://doi.org/10.1007/s10933-006-9074-x

Kim, S.T., O’Neil, J.R., 1997. Equilibrium and nonequilibrium oxygen isotope effects in synthetic carbonates. Geochimica et Cosmochimica Acta 61, 3461–3475. https://doi.org/10.1016/S0016-7037(97)00169-5

Larocque, I., Finsinger, W., 2008. Late-glacial chironomid-based temperature reconstructions for Lago Piccolo di Avigliana in the southwestern Alps (Italy). Palaeogeography, Palaeoclimatology, Palaeoecology 257, 207–223. https://doi.org/10.1016/j.palaeo.2007.10.021

Laskar, J., Robutel, P., Joutel, F., Gastineau, M., Correia, A.C.M., Levrard, B., 2004. A long-term numerical solution for the insolation quantities of the Earth. A&A 428, 261–285. https://doi.org/10.1051/0004-6361:20041335

Li, X., Liu, W., 2010. Oxygen isotope fractionation in the ostracod Eucypris mareotica: results from a culture experiment and implications for paleoclimate reconstruction. J Paleolimnol 43, 111–120. https://doi.org/10.1007/s10933-009-9317-8

Lionello, P., Scarascia, L., 2018. The relation between climate change in the Mediterranean region and global warming. Reg Environ Change 18, 1481–1493. https://doi.org/10.1007/s10113-018-1290-1

Ludovisi, A., Gaino, E., 2010. Meteorological and water quality changes in Lake Trasimeno (Umbria, Italy) during the last fifty years. J Limnol 69, 174. https://doi.org/10.4081/jlimnol.2010.174

Magny, M., Peyron, O., Sadori, L., Ortu, E., Zanchetta, G., Vanniere, B., Tinner, W., 2012 Contrasting patterns of precipitation seasonality during the Holocene in the south- and north-Central Mediterranean Journal of Quaternary Science, 27, 290-296

Marchegiano M., Peral M., Venderickx J., Martens K., García-Alix A., Snoeck, C. Goderis S., and Claeys P. The ostracod clumped-isotope thermometer: A novel tool to reconstruct quantitative continental climate changes. Eartharxiv https://doi.org/10.31223/X5T967

Marchegiano, M., Gliozzi, E., Ceschin, S., Mazzini, I., Adatte, T., Mazza, R., Ariztegui, D., 2017. Ecology and distribution of living ostracod assemblages in a shallow endorheic lake: the example of the Lake Trasimeno (Umbria, central Italy). J Limnol. https://doi.org/10.4081/jlimnol.2017.1478

Marchegiano, M., Francke, A., Gliozzi, E., Ariztegui, D., 2018. Arid and humid phases in central Italy during the Late Pleistocene revealed by the Lake Trasimeno ostracod record. Palaeogeography, Palaeoclimatology, Palaeoecology 490, 55–69. https://doi.org/10.1016/j.palaeo.2017.09.033

Marchegiano, M., Francke, A., Gliozzi, E., Wagner, B., Ariztegui, D., 2019. High-resolution palaeohydrological reconstruction of central Italy during the Holocene. The Holocene 29, 481–492. https://doi.org/10.1177/0959683618816465

Marchegiano, M., Horne, D.J., Gliozzi, E., Francke, A., Wagner, B., Ariztegui, D., 2020. Rapid Late Pleistocene climate change reconstructed from a lacustrine ostracod record in central Italy (Lake Trasimeno, Umbria). Boreas 49, 739–750. https://doi.org/10.1111/bor.12450

Marchegiano, M., John, C.M., 2022. Disentangling the Impact of Global and Regional Climate Changes During the Middle Eocene in the Hampshire Basin: New Insights From Carbonate Clumped Isotopes and Ostracod Assemblages. Paleoceanog and Paleoclimatol 37. https://doi.org/10.1029/2021PA004299

Marchegiano M., Peral M., Venderickx J., Martens K., Garcia-Alix A., Snoeck C., Goderis S., and Claeys P. (2023) The ostracod clumped isotope thermometer: A novel tool to reconstruct quantitative continental climate changes. Preprint https://eartharxiv.org/repository/view/5752/

Marino G, Rohling EJ, Sangiorgi F, et al. 2009. Early and middle Holocene in the Aegean Sea: interplay between high and low latitude climate variability. Quaternary Science Reviews 28: 3246–3262

Martin-Puertas, C., Valero-Garces, B.L., Pilar Mata, M., Gonzalez-Samperiz, P., Bao, R., Moreno, A., Stefanova, V., 2008. Arid and humid phases in southern Spain during the last 4000 years: the Zonar Lake record, Cordoba. The Holocene 18, 907–921. http://dx.doi.org/10.1177/0959683608093533.

Meinicke, N., Reimi, M.A., Ravelo, A.C., Meckler, A.N., 2021. Coupled Mg/Ca and Clumped Isotope Measurements Indicate Lack of Substantial Mixed Layer Cooling in the Western Pacific Warm Pool During the Last ~5 Million Years. Paleoceanogr Paleoclimatol 36. https://doi.org/10.1029/2020PA004115

Meisch, C. (Ed.), 2000. Ostracoda, Süßwasserfauna von Mitteleuropa / begr. von A. Brauer. Hrsg. von J. Schwoerbel. Spektrum Akad. Verl, Heidelberg Berlin.

Peyron O, Goring S, Dormoy I, et al. 2011. Holocene seasonality changes in the central Mediterranean region reconstructed from the pollen sequences of Lake Accesa (Italy) and Tenaghi Philippon (Greece). The Holocene 21: 131–147.

Peral, M., Blamart, D., Bassinot, F., Daëron, M., Dewilde, F., Rebaubier, H., Nomade, S., Girone, A., Marino, M., Maiorano, P., Ciaranfi, N., 2020. Changes in temperature and oxygen isotopic composition of Mediterranean water during the Mid-Pleistocene transition in the Montalbano Jonico section (southern Italy) using the clumped-isotope thermometer. Palaeogeography, Palaeoclimatology, Palaeoecology 544, 109603. https://doi.org/10.1016/j.palaeo.2020.109603

Rasmussen, T.L., Thomsen, E., Moros, M., 2016. North Atlantic warming during Dansgaard-Oeschger events synchronous with Antarctic warming and out-of-phase with Greenland climate. Sci Rep 6, 20535. https://doi.org/10.1038/srep20535

Reimer, P.J., 2020. Composition and consequences of the IntCal20 radiocarbon calibration curve. Quat. res. 96, 22–27. https://doi.org/10.1017/qua.2020.42

Roberts, L.R., Holmes, J.A., Horne, D.J., 2020. Tracking the seasonal calcification of Cyprideis torosa (Crustacea, Ostracoda) using Mg/Ca-inferred temperatures, and its implications for palaeotemperature reconstruction. Marine Micropaleontology 156, 101838. https://doi.org/10.1016/j.marmicro.2020.101838

Robles, M., Peyron, O., Ménot, G., Brugiapaglia, E., Wulf, S., Appelt, O., Blache, M., Vannière, B., Dugerdil, L., Paura, B., Ansanay-Alex, S., Cromartie, A., Charlet, L., Guédron, S., de Beaulieu, J.-L., Joannin, S., 2023. Climate changes during the Late Glacial in southern Europe: new insights based on pollen and brGDGTs of Lake Matese in Italy. Clim. Past 19, 493–515. https://doi.org/10.5194/cp-19-493-2023

Samartin, S., Heiri, O., Joos, F., Renssen, H., Franke, J., Brönnimann, S., Tinner, W., 2017. Warm Mediterranean mid-Holocene summers inferred from fossil midge assemblages. Nature Geosci 10, 207–212. https://doi.org/10.1038/ngeo2891

Song, B., Zhang, K., Farnsworth, A., Ji, J., Algeo, T.J., Li, X., Xu, Y., Yang, Y., 2022. Application of ostracod-based carbonate clumped-isotope thermometry to paleo-elevation reconstruction in a hydrologically complex setting: A case study from the northern Tibetan Plateau. Gondwana Research 107, 73–83. https://doi.org/10.1016/j.gr.2022.02.014

Tarutani, T., Clayton, R.N., Mayeda, T.K., 1969. The effect of polymorphism and magnesium substitution on oxygen isotope fractionation between calcium carbonate and water. Geochimica et Cosmochimica Acta 33, 987–996. https://doi.org/10.1016/0016-7037(69)90108-2

Toney, J.L., García-Alix, A., Jiménez-Moreno, G., Anderson, R.S., Moossen, H., Seki, O., 2020. New insights into Holocene hydrology and temperature from lipid biomarkers in western Mediterranean alpine wetlands. Quaternary Science Reviews 240, 106395. https://doi.org/10.1016/j.quascirev.2020.106395

Turpen, J.B., Angell R.W., 1971. Aspects of moulting and calcification in the ostracode Heterocypris. The Biological Bulletin 140, 331–338.

Yue, J., Xiao, J., Wang, X., Meckler, A.N., Modestou, S.E., Fan, J., 2022. “Cold and wet” and “warm and dry” climate transitions at the East Asian summer monsoon boundary during the last deglaciation. Quaternary Science Reviews 295, 107767. https://doi.org/10.1016/j.quascirev.2022.107767

World Lake Database 2013, International Lake Environment Committee Foundation. https://wldb.ilec.or.jp

FIGURE AND TABLE CAPTIONS

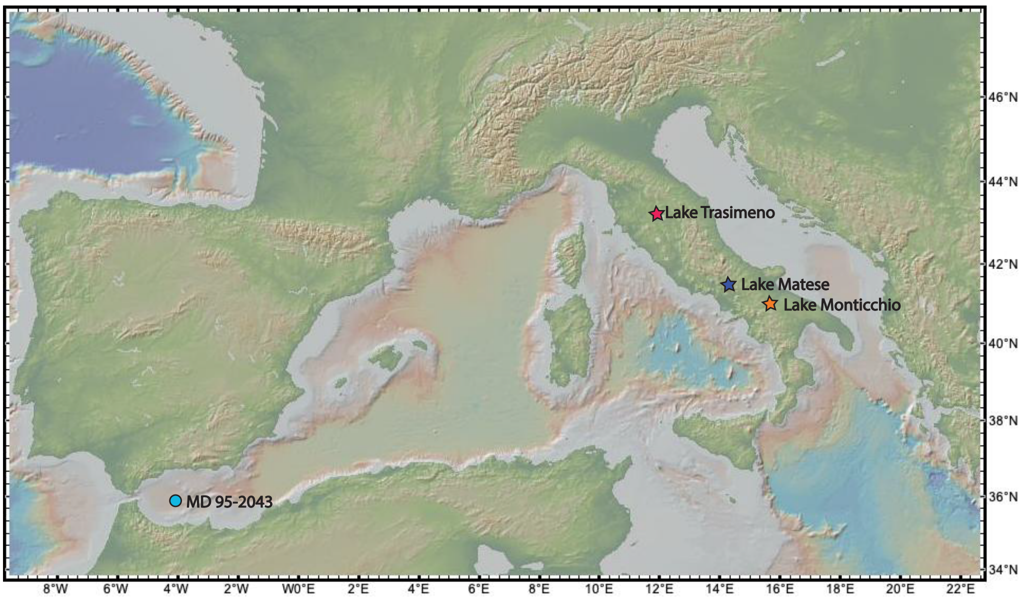

Fig. 1: Location of the records discussed in this study. Marine record MD 95-2043 from Alboran Sea (Cacho et al., 1999). Lacustrine records from Lake Trasimeno (this study), Lake Matese (Robles et al., 2023) and Lake Monticchio (Allen et al., 1999)

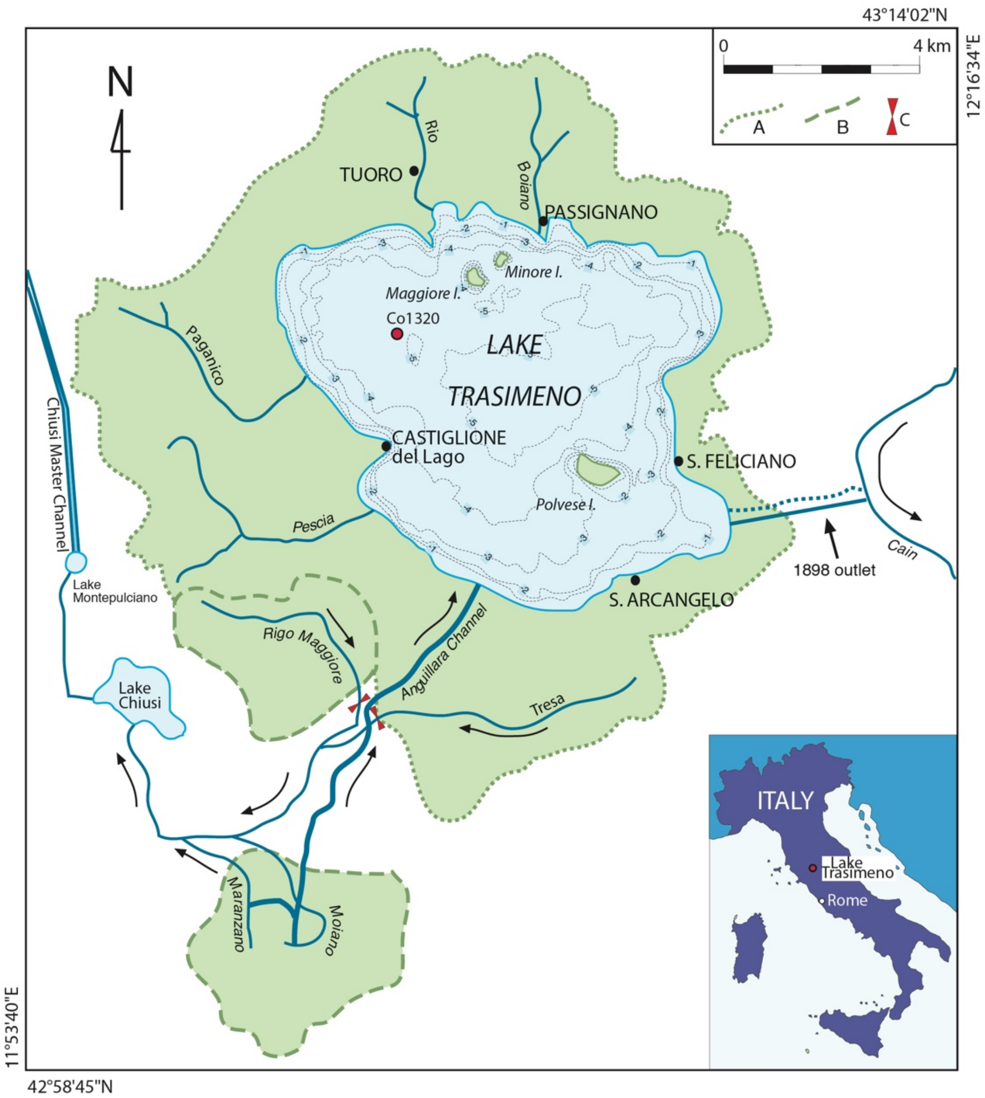

Fig. 2: Lake Trasimeno and core location, modified from Marchegiano et al. (2018). A, Natural catchment area; B, artificially-joined basins; C, sluice gates of the artificially-joined channels.

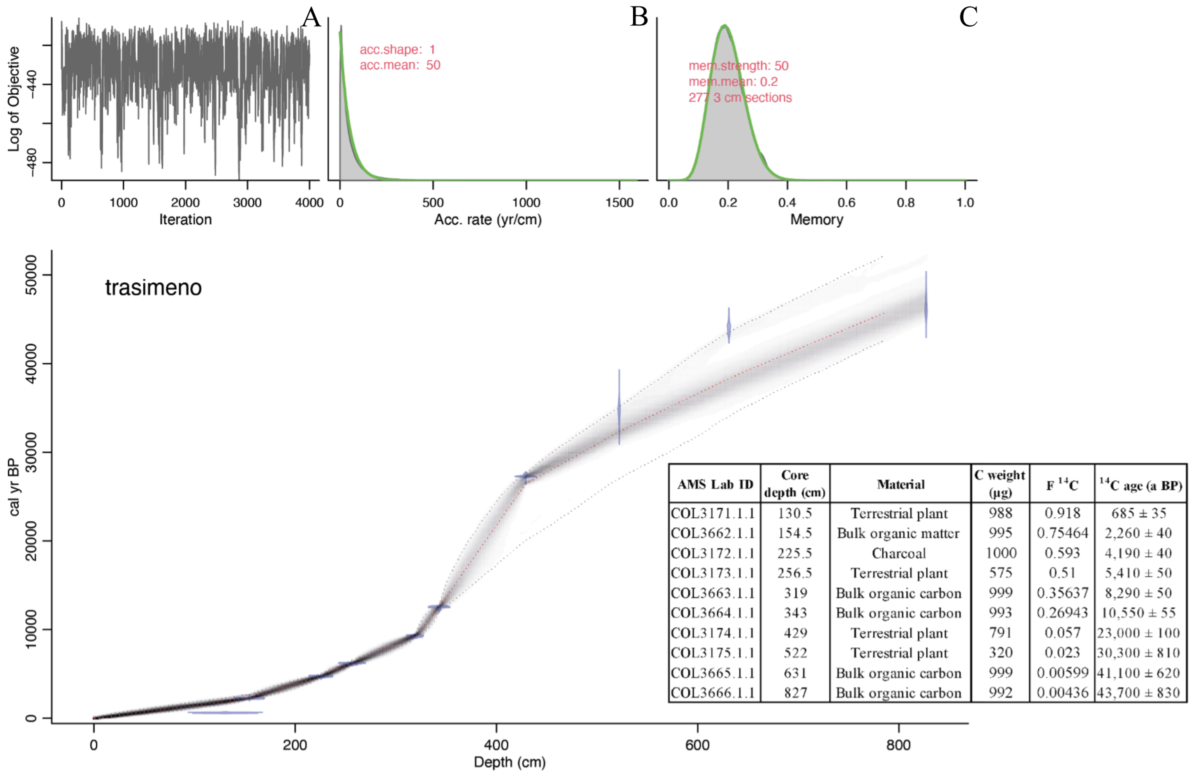

AMS Lab ID	Core depth (cm)	Material	C weight (µg)	F ^{14}C	^{14}C age (a BP)
COL3171.1.1	130.5	Terrestrial plant	988	0.918	685 ± 35
COL3662.1.1	154.5	Bulk organic matter	995	0.75464	2,260 ± 40
COL3172.1.1	225.5	Charcoal	1000	0.593	4,190 ± 40
COL3173.1.1	256.5	Terrestrial plant	575	0.51	5,410 ± 50
COL3663.1.1	319	Bulk organic carbon	999	0.35637	8,290 ± 50
COL3664.1.1	343	Bulk organic carbon	993	0.26943	10,550 ± 55
COL3174.1.1	429	Terrestrial plant	791	0.057	23,000 ± 100
COL3175.1.1	522	Terrestrial plant	320	0.023	30,300 ± 810
COL3665.1.1	631	Bulk organic carbon	999	0.00599	41,100 ± 620
COL3666.1.1	827	Bulk organic carbon	992	0.00436	43,700 ± 830

Fig. 3: Chronology of the Trasimeno core. The chronology is based on radiocarbon ages from Marchegiano et al., (2018) modelled with Bayesian statistics using Bacon 3.1 0 by Blaauw & Christen (2011) and IntCal 2020 (Reimer et al. 2020). A, Markov Chain Monte Carlo (MCMC) iterations; B, prior (green) and posterior (grey histogram) distribution for the accumulation sedimentation rate (years/cm); C, memory.

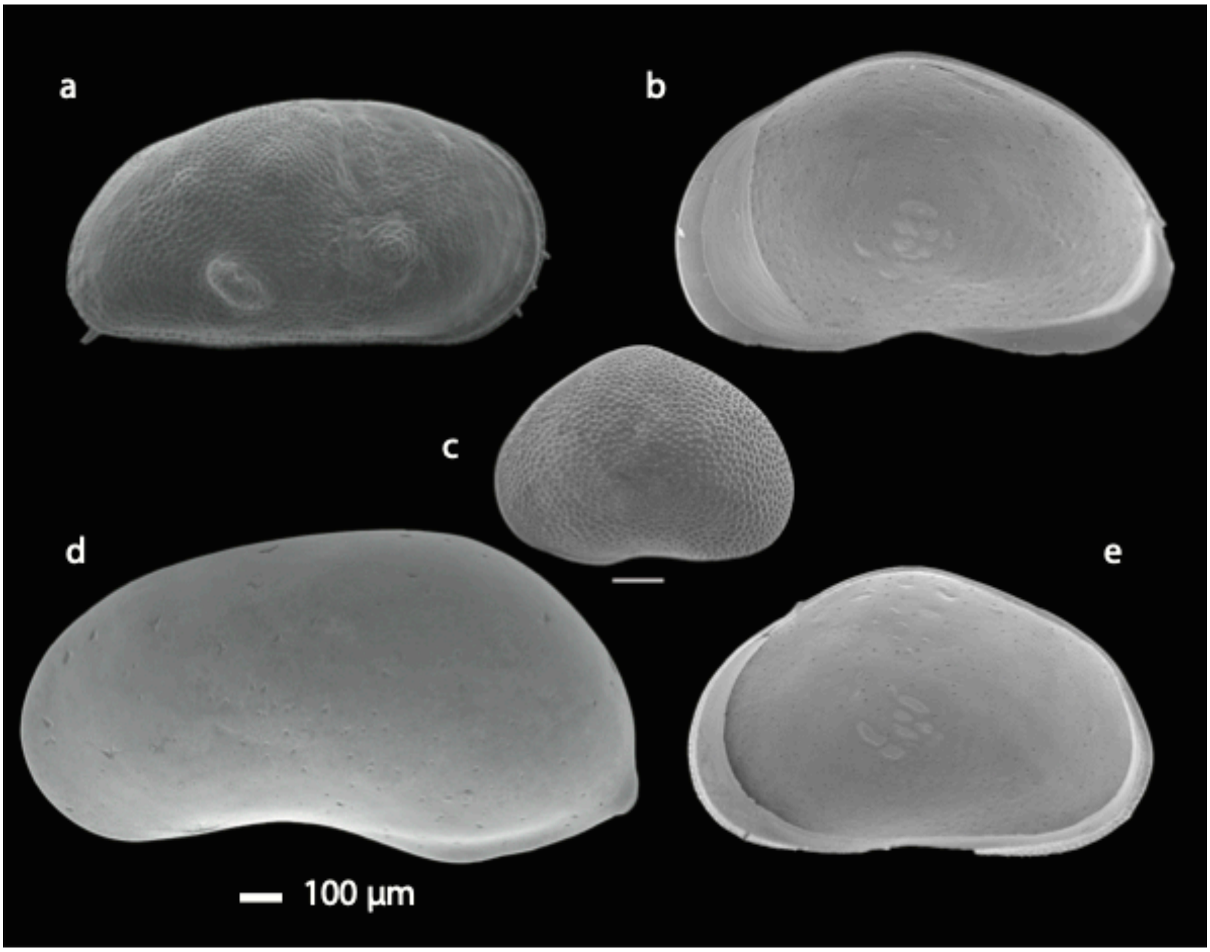

Fig. 4: Ostracod SEM pictures, made at the University of Roma Tre, obtained from samples of the Lago Trasimeno Co1320 core, a. *Cyprideis torosa*, b, *Eucypris mareotica*, c, *Sarcypridopsis aculeata*, d, *Candona angulata* and e, *Heterocypris salina.*

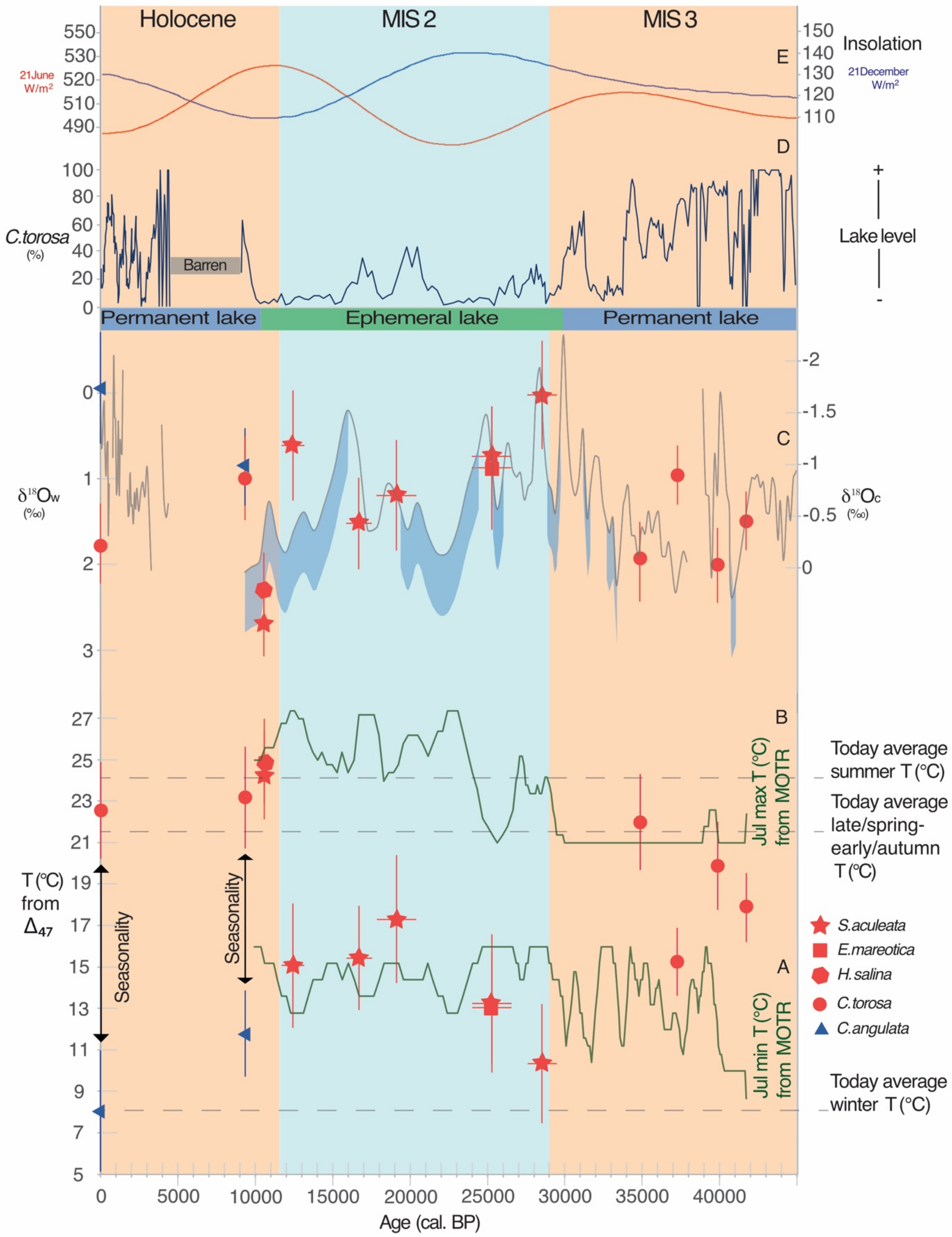

Fig. 5: Clumped isotope temperature and reconstructed $\delta^{18}O_w$ (this study) from the most abundant species *Cyprideis torosa*, *Eucypris mareotica*, *Sarcypridopsis aculeata*, *Candona*

angulata and *Heterocypris salina* (red and blue symbols: red symbols, warm season species; blue symbols, cold season species). Mutual Ostracod Temperature Range (MOTR, from Marchegiano et al., 2020) A (Jul min) and B (Jul max) curves, bulk carbonate $\delta^{18}O$ data of Lago Trasimeno from Francke et al. (2022) (C black line,), the uncertainty in certain carbonate samples (blue shade) is due to the mixed composition of aragonite/calcite and the subsequent application of different correction factors (+0.6 for the aragonite, Tarutani et al., 1969) (Francke et al., 2022); $\delta^{18}O_w$ reconstructed from ostracod shells (red and blue symbols: red symbols, warm season species; blue symbols, cold season species), *C. torosa* ostracod abundance used to reconstruct lake level variations (D curve) (Marchegiano et al., 2018) and summer and winter insolation (E curve) (Laskar et al., 2004). Present mean water winter, late spring/early autumn and summer temperature are indicated.

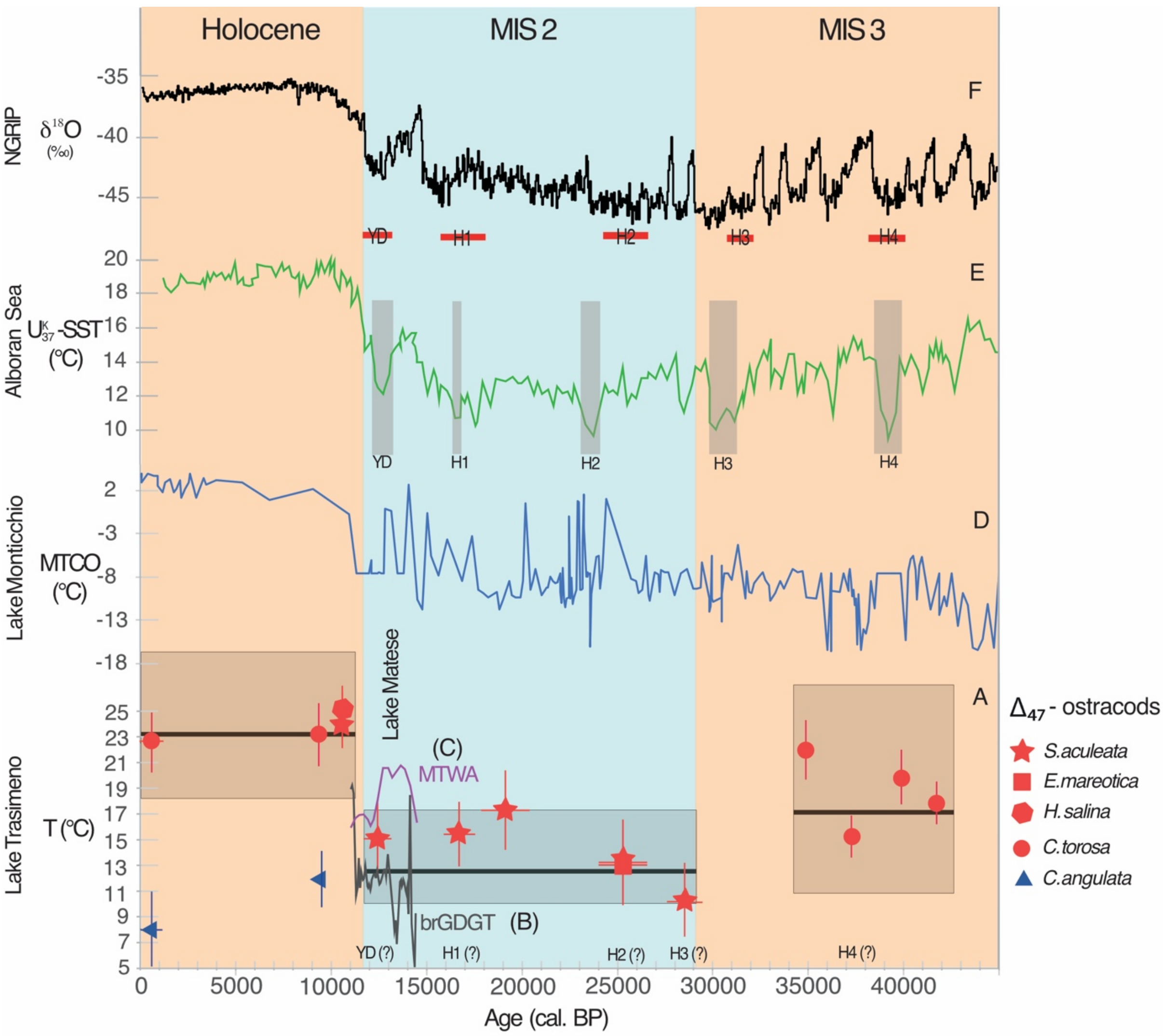

Fig. 6: Paleotemperature reconstruction at Lake Trasimeno and comparison with other Mediterranean records (A). Box plots for Δ_{47} temperatures, including all replicate measurements per each samples (see Table 1 in supplementary material), show median (black bold line), the first (25%) and third quartiles (75%, i.e. the grey box covers 50% of the probability density function) (A), brGDGT mean annual (B) and pollen reconstructed mean temperatures of the warmest month (MTWA) (C) from Lake Matese (Robles et al., 2023), pollen reconstructed mean temperatures of the coldest month (MTCO) from Lake Monticchio (D) (Allen et al., 1999) alkenones marine surface annual mean temperature from Alborean Sea (E) (Cacho et al., 1999) and the $\delta^{18}O$ from the North Greenland Ice Core Project (F) (Rasmussen et al., 2016).

Sample name	Depth (cm)	n°. replicates	Δ_{47} (‰)	Δ_{47} (‰) (1SE)	Δ_{47}-T (2SE)	δ13C (‰)	δ18O (‰)	Specie	Vital offset (‰)	δ18Ocorr (‰) (VPDB)	δ18Ow (‰)	δ18Ow (‰) SE	Average age (ky. cal BP)	Age
TRAR1	14-83	6	0.648	0.0144	8.0 ± 2.9	-0.49	3.13	C. angulata	-2.2	0.93	-0.1	0.326	0.7	HOLOCENE
TRAR2	14-83	10	0.601	0.0111	22.5 ± 2.3	-3.17	0.42	C. torosa	-0.8	-0.38	1.7	0.234	0.7	
TRAHOL1	316-322	9	0.599	0.0115	23.1 ± 2.5	-0.28	-0.45	C. torosa	-0.8	-1.25	1.0	0.248	9	
TRAHOL2	316-322	10	0.636	0.0111	11.8 ± 2.1	2.17	3.20	C. angulata	-2.2	1.00	0.9	0.226	9	
TRA2	328-330	12	0.594	0.0101	24.9 ± 2.0	3.99	0.03	S. aculeata	0	0.03	2.7	0.202	10.5	
TRA2B	328-330	11	0.596	0.0105	24.3 ± 2.2	3.60	-0.21	H. salina	0	-0.21	2.3	0.215	10.5	
TRAGI1	336-348	6	0.625	0.0140	15.1 ± 3.0	2.54	0.05	S. aculeata	0	0.06	0.6	0.321	12	LGM-MIS2
TRAH1	363-375	8	0.623	0.0123	15.4 ± 2.5	3.50	0.86	S. aculeata	0	0.86	1.5	0.267	17	
TRAGS2	375-393	6	0.617	0.0140	17.3 ± 3.1	3.58	0.15	S. aculeata	0	0.15	1.2	0.323	19	
TRAH2-1	413-431	7	0.631	0.0131	13.0 ± 2.7	3.09	0.61	S. aculeata	0	0.61	0.7	0.290	25	
TRAH2-2	413-431	5	0.631	0.0153	13.2 ± 3.3	1.70	0.69	E. mareotica	0	0.70	0.9	0.360	25	
LATEMIS3	445-477	6	0.640	0.0140	10.3 ± 2.9	0.10	0.50	S. aculeata	0	0.50	0.0	0.316	28	
TRA4	561-569	10	0.603	0.0111	22.0 ± 2.3	-1.32	0.74	C. torosa	-0.8	-0.06	2.0	0.233	35	BLGM-MIS3
TRA5	603-616	14	0.624	0.0094	15.2 ± 1.6	-0.47	1.15	C. torosa	-0.8	0.35	1.0	0.173	37	
TRA6	658-654	11	0.609	0.0107	19.9 ± 2.1	0.64	1.21	C. torosa	-0.8	0.41	2.0	0.219	40	
TRA7	732-748	14	0.616	0.0093	17.9 ± 1.7	-3.47	1.12	C. torosa	-0.8	0.32	1.5	0.171	42	

Table 1: Carbonate classic and clumped isotopes results. The Δ_{47}-T are calculated using the unified calibration (Anderson et al., 2021) and the $\delta^{18}O_w$ calculated from Δ_{47} and $\delta^{18}O_{ost}$ data using the formula of Kim and O'Neal (1997). BLGM: Before Last Glacial Maximum; LGM: Last Glacial Maximum.

SPECIES	CALCIFICATION SEASON	AGE	SAMPLE	Δ_{47}-T (2SE)	TODAY AVERAGE SEASON WATER-T
C. torosa	late-spring/early-autumn	HOLOCENE	TRAR2	22,5 ± 2.3	21.4
			TRAHOL1	23,1 ± 2.5	21.4
		BLGM-MIS3	TRA4	22 ± 2.3	21.4
			TRA5	15,2 ± 1.6	21.4
			TRA6	19,9 ± 2.1	21.4
			TRA7	17,9 ± 1.7	21.4
S. aculeata	summer	HOLOCENE	TRA2	24,9 ± 2	24
		LGM-MIS2	TRAGI1	15,1 ± 3	24
			TRAH1	15,4 ± 2.5	24
			TRAGS2	17,3 ± 3.1	24
			TRAH2-1	13,0 ± 2.7	24
			LATEMIS3	10,3 ± 2.9	24
E. mareotica	summer	LGM-MIS2	TRAH2-2	13,2 ± 3.3	24
H. salina	summer	HOLOCENE	TRA2B	24,3 ± 2.2	24
C. angulata	winter	HOLOCENE	TRAR1	8 ± 2.9	8
			TRAHOL2	11,8 ± 2.1	8

Table 2: Ostracod species used for Δ_{47} – T reconstruction, their shell calcification season *(C. torosa*, from Heip, 1976, Roberts et al., 2020 and consideration from this study; *S. aculeata* Meisch et al., 2000; *E. mareotica*, Li and Liu, 2010; *H. salina*, Meisch et al., 2000; *C. angulata,* Meisch et al., 2000) and present average seasonal Lake Trasimeno water temperatures (World Lake database 2023)